Size Exclusion Chromatography in Pore Networks

C. McGreavy[1]* / J. S. Andrade Junior[2] / K. Rajagopal[2]

[1]Department of Chemical Engineering, The University of Leeds, Leeds LS2-9JT, UK
[2]Programa de Engenharia Quimica, COPPE Universidade Federal do Rio de Janeiro CP 68502, Rio de Janeiro, RJ, Brasil

Key Words

Summary

A network model is proposed to describe the intraparticle porous structure of an SEC (size exclusion chromatography) column and solved using orthogonal collocation. Comparison of the retention and band broadening features with the conventional model of a parallel bundle of capillaries shows significant differences, which demonstrate the importance of including morphological characteristics into the model to account for the mass transfer restrictions.

Introduction

Size exclusion chromatography (SEC) has been largely employed as an analytical procedure for separating macromolecules according to differences in size and in obtaining information on the molecular weight distribution of polymers [1]. A number of theoretical models have been proposed in the literature for describing the basic mechanistic processes [2–4]. Basically it is concerned with hindered diffusion [5] in a disordered porous medium such as the intraparticle pore volume of the column packing. The majority of studies in this field [6–7] have been developed assuming that a homogeneous macroscopic model based on an overall effective diffusion coefficient can provide a match between model predictions and experimental data. Much less effort has been devoted to improve the structural description of the intraparticle morphology. Recently, Sahimi and Jue [8–9] introduced a network model to represent the diffusion of macromolecules in randomly structured porous media. Computer simulations showed that the topology of the pore volume plays a significant role in determining the mass transport process.

The main objective of the present work is to apply the network modelling technique to the investigation of the influence of the pore volume morphology on the SEC mechanisms related to *retention* and *band broadening*. A parallel bundle of capillaries is taken as a conceptual reference model so as to illustrate the importance of the pore interconnectivity as a network topological feature.

Physico-Chemical System

The conceptual physico-chemical description of the system is based on the following assumptions:

a) The chromatographic column is represented by a fixed bed packed with porous particles of uniform size.

b) The polymer samples used as tracers are assumed to have a very narrow molecular weight distribution, i.e. they are *standard samples*. To illustrate the approach, data related to polystyrene in chloroform will be used. Correlations [7] for the root mean square radius of gyration (R_p) and the molecular diffusion (D_m^0) of the polymer as a function of its molecular weight (MW) are given by:

$$R_p = 0.0150 \times 10^{-7}\, MW^{0.581} \tag{1}$$

and

$$D_m^0 = 1.61 \times 10^{-4}\, MW^{-0.525}$$
$$MW \leq 38\,000 \tag{2}$$
$$D_m^0 = 3.72 \times 10^{-4}\, MW^{-0.577}$$
$$MW \geq 110\,000 \tag{3}$$

at 20 °C.

Axial dispersion (D_L) is regarded as being significant and dependent on the molecular weight of the polymer. For the system used here a theoretical correlation developed in [10] is employed. All the relevant parameters are listed in Table I.

c) The porous particles are structurally represented by two different models (Figure 1):

Table I. Parameters employed in the simulations (from reference [13]).

Column parameters	
length (L)	121.2 cm
interstitial velocity ($\langle v \rangle$)	0.0958 cm/s
porosity (ε_c)	0.364
Particle parameters	
size (l_p)	0.003 cm
small radius (R_1)	10^{-6} cm
large radius (R_2)	3×10^{-6} cm
porosity (ε_p)	0.616

a)

b)

Figure 2

a) Network lattice with the nodal enumeration scheme employed in the simulations.

b) Schematic representation of the SEC column showing the collocation points and the network lattice employed in the simulations.

Figure 1

Pore volume representations of the porous particles in a SEC column.

(i) – a 20×20 two dimensional square network made up of cylindrical pores of constant length (l) connected to sites or nodes of negligible volume.

(ii) – a parallel bundle of cylindrical capillaries.

d) By fixing the frequency of the smaller radius (F1), two different radius sizes (R_1 and R_2) can be assigned to the parallel bundle and the network pore radii. In the network case, the spatial arrangement of both types of capillaries is generated using a routine for random permutation of vectors.

Mathematical Formulation

Particle Model

Figure 2a shows the lattice representation of the network with the nodal enumeration scheme adopted in this work. In a typical pore between nodes {i} and {j}, the tracer concentration ($\bar{c}(x, t)$) is described by the following mass balance:

$$\frac{\partial \bar{c}}{\partial t} = D_m \frac{\partial^2 \bar{c}}{\partial x^2} \qquad (4)$$
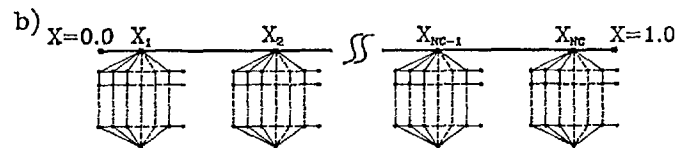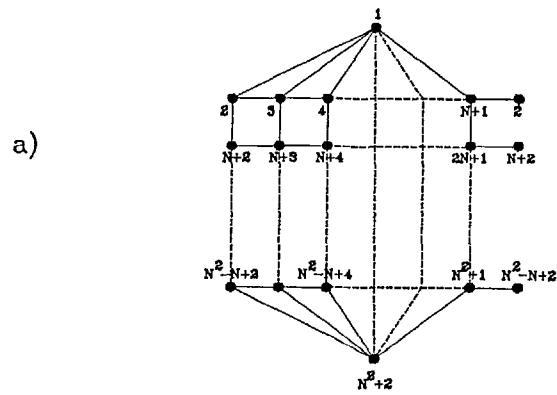
where D_m is the *hindered* molecular diffusion coefficient and x is the axial coordinate in any particular capillary between nodes {i} and {j} of the network, where {i} is the origin with respect to the local value of x, i.e. each capillary is treated separately. Assuming that the polymer molecules interact with the capillary pore wall by a *hard sphere* potential, the following expression given by Pappenheimer et al. [11] can be used to evaluate D_m:

$$D_m = D_m^0 (1 - 2.1044\lambda + 2.0888\lambda^3 - 0.948\lambda^5) \qquad (5)$$

where $\lambda = R_p/R$.

The corresponding boundary conditions are introduced in a convenient form by using the Laplace transform with respect to time in Eq. (4):

$$sc - D_m \frac{d^2 c}{dx^2} = 0 \qquad (6)$$

assuming that there is no tracer species inside the pore initially, i.e. $\bar{c}(x, 0) = 0$. The transformed form for the boundary conditions is then:

$$c(0, s) = c_{\{i\}}$$
$$c(l, s) = c_{\{j\}} \qquad (7)$$

Solving Eq. (6) subject to the boundary conditions (7):

$$c(x, s) = \frac{\sinh(ax)}{\sinh(al)} c_{\{j\}}$$
$$+ \left[\cosh(ax) - \frac{\sinh(ax)}{\tanh(al)} \right] c_{\{i\}} \qquad (8)$$

where $a = (s/D_m)^{1/2}$.

The transformed form of the molar flux of the tracer into a pore from adjacent sites {i} and {j} can be written as:

$$J_{\{i,j\}} = -\Pi R_{\{i,j\}}^2 \phi D_m \left(\frac{dc}{dx}\bigg|_{x=0}\right)_{\{i,j\}} \qquad (9)$$

where ϕ is the partitioning or distribution coefficient, the ratio of the average intrapore concentration to the bulk solution concentration, for a single capillary at equilibrium. For purely steric interactions between the solute and pore wall it follows [1] that:

$$\phi = (1-\lambda)^2 \qquad (10)$$

Then, $J_{\{i,j\}}$ can be expressed as a linear function of the two terminal transformed concentrations at the connected nodal points:

$$J_{\{i,j\}} = \Pi R_{\{i,j\}}^2 \phi (D_{ms})^{1/2} \left[\frac{c_{\{i\}}}{\tanh(al)} - \frac{c_{\{j\}}}{\sinh(al)}\right] \qquad (11)$$

The nodes are considered to be points of perfect mixing. Imposing the conservation of mass at each internal node by setting the algebraic sum of the fluxes to zero, for the node {i}, this can be expressed in terms of the transformed representation as:

$$J_{\{i,i-N\}} + J_{\{i,i-1\}} + J_{\{i,i+1\}} + J_{\{i,i+N\}} = 0 \qquad (12)$$

For a tube of the parallel bundle, the hindered mass transport is described by the same mathematical formulation derived above for the network capillary. The length of the capillary in the network is defined by:

$$l = l_p/(N+1)$$

but the particle size itself (l_p) is utilized as the capillary length in the simulations based on the parallel bundle. To complete the description of the net flux to/from the network, a mass conservation equation for all the connection nodes at the end of the structure must also be included at $\{N^2 + 2\}$ (see Figure 2a). This is the only nodal mass balance needed for the parallel bundle case.

Column Model

A simple mass balance in the mobile phase of the *SEC* column gives:

$$D_L \frac{\partial^2 \overline{C}_m}{\partial X^2} - \langle v \rangle \frac{\partial \overline{C}_m}{\partial X} - \frac{\partial \overline{C}_m}{\partial t}$$
$$- \frac{(1-\epsilon_c)\epsilon_p}{\epsilon_c V_{PS}} \sum_{j=2}^{N+1} \overline{J}_{\{1,j\}} = 0 \qquad (13)$$

where D_L is the column dispersion coefficient, $\langle v \rangle$ represents the fluid intersticial velocity, V_{PS} is the internal volume of the particle pore volume and ϵ_c and ϵ_p are the column and particle porosities respectively. The factor

$$\frac{(1-\epsilon_c)\epsilon_p}{\epsilon_c V_{PS}}$$

in the flux summation term of Eq. (13) corresponds to the reciprocal of the external fluid volume sur-

rounding a single particle in the mobile phase. It is assumed that the particle porous structure repeats itself in the axial direction of the fixed bed and so the same network configuration is applied over the whole range of X values. Initially, the bed is taken to be free of solute:

$$\overline{C}_m(X, 0) = 0 \qquad (14)$$

with the following boundary conditions holding for the entrance and the exit of the column:

$$\langle v \rangle \delta(t) = \langle v \rangle \overline{C}_m(0, t) - D_L \frac{\partial \overline{C}_m}{\partial X}\bigg|_{X=0} \qquad (15)$$

$$\frac{\partial \overline{C}_m}{\partial X}\bigg|_{X=L} = 0 \qquad (16)$$

where $\delta(t)$ is the Dirac function.

Introducing the Laplace transform of the mobile phase concentration (C_m):

$$C_m(X, s) = \int_0^\infty \overline{C}_m(X, t) \exp(-st) \, dt$$

then:

$$D_L \frac{\partial^2 C_m}{\partial X^2} - \langle v \rangle \frac{\partial C_m}{\partial X} - s C_m - \frac{(1-\epsilon_c)\epsilon_p}{\epsilon_c V_{PS}} \sum_{j=2}^{N+1} J_{\{1,j\}} = 0 \qquad (17)$$

with:

$$\frac{\partial C_m}{\partial X}\bigg|_{X=0} = \langle v \rangle (C_m(0,s) - 1)/D_L \qquad (18)$$

and

$$\frac{\partial C_m}{\partial X}\bigg|_{X=L} = 0 \qquad (19)$$

At any time, assuming that the mobile phase concentration is equal to nodal concentration at the network entrance, the following equation provides the connection between the mobile phase and the intraparticle pore volume:

$$\overline{C}_m = \overline{c}_{\{1\}} \qquad (20)$$

Combining Eqs. (17)–(20) and the internal site mass balances (Eq. (12)) together with the expression for the transformed form of the molar flux in each capillary (Eq. (11)), a complete description of the whole system is obtained.

Numerical Solution

For a fixed value of the transformed variable (s), the mobile phase Eq. (17) is discretized using orthogonal collocation [12]. The normalized orthogonal collocation points employed are the zeros of the Jacobi polynomial $P_{N_c}^{(0,0)}$ and the boundaries $(X/L = 0$ and $X/L = 1)$ are taken as interpolation points. A schematic representation of the collocation procedure for

axial discretization of the system is shown in Figure 2b. The resulting system of linear algebraic equations is conveniently expressed in matrix form as:

$$AC = B \qquad (21)$$

where C is the vector of transformed concentrations, B is the *input* vector obtained from Eq. (18) and A is a *conductance matrix* corresponding to the coupling between the internal site mass balances of the network and the orthogonal collocation coefficients (Figure 3).

This system of equations is conveniently solved numerically using *LU-decomposition* of real sparse matrices. The prodecure is then repeated for different s values from which calculated transformed concentrations at the column exit ($C_m(L, s)$) are obtained.

The first and second moments of the residence time distribution are then computed by numerical differentiation using:

$$\mu_1 = RT = -\left.\frac{\partial C_m(L, s)}{\partial s}\right|_{s = 0} \qquad (22)$$

$$\mu_2 = \left.\frac{\partial^2 C_m(L, s)}{\partial s^2}\right|_{s = 0} \qquad (23)$$

where RT is the polymer retention time. The standard deviation of the elution curve is obtained as:
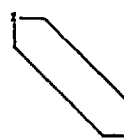
$$SD = (\mu_2 - \mu_1^2)^{1/2} \qquad (24)$$
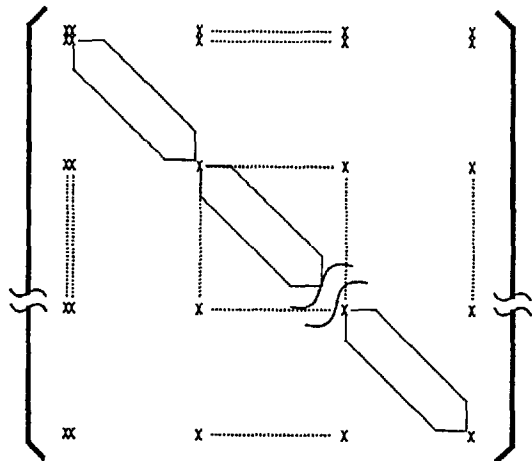
Figure 3
Schematic representation of matrix A.

The approximation order Nc of the orthogonal polynomials (i.e. the number of orthogonal collocation points) for the mobile phase Eq. (17) has been examined for Nc = 3, 4, 5, 6. Comparison with the higher order approximations shows Nc = 4 to be adequate for obtaining relative errors smaller than 0.01 % of the first moment and 0.1 % of the standard deviation. For a fixed polymer molecular weight and a small radius frequency (F1), 40 simulations with distinct network samples have been carried out, from which average values for the first and second moments have been obtained.

Results and Discussion

The Figures 4 and 5 show the *calibration* curves for different values of F1 for the parallel bundle and the network models respectively. The retention time (RT)
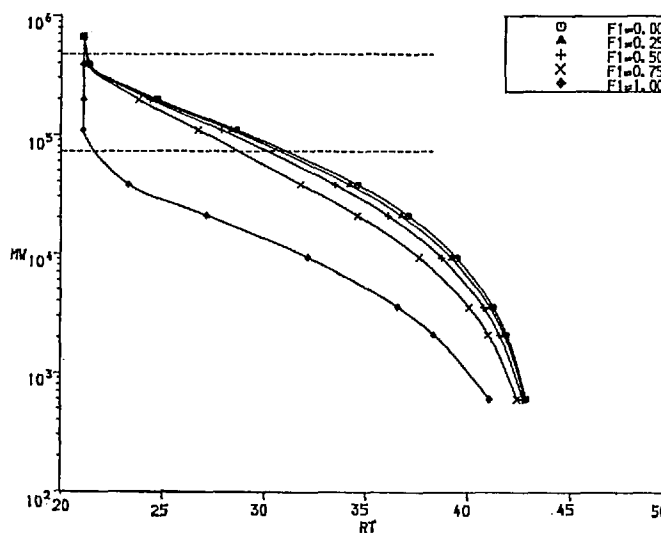

Figure 4
Calibration curves using the parallel bundle as the intraparticle pore volume model (RT in minutes).
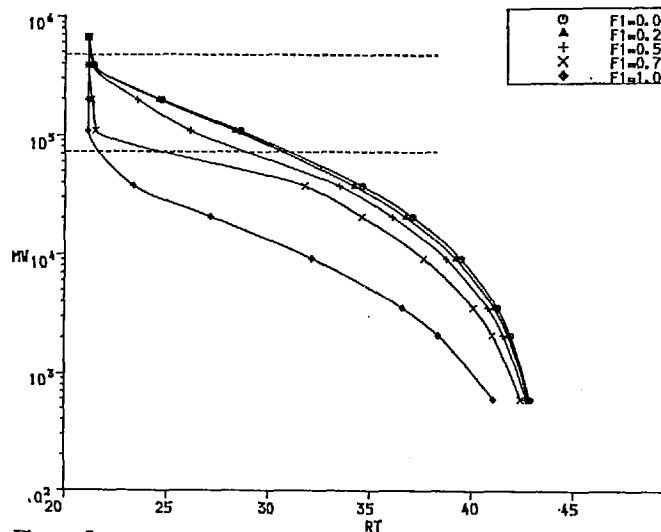

Figure 5
Calibration curves using the network as the intraparticle pore volume model (RT in minutes).

depends on the exclusion mechanism. For a fixed polymer molecular weight, it decreases as F1 increases. Also, as the polymer molecular weight increases the elution retention time decreases, tending to the total exclusion limit.

The dashed lines represent the polymer molecular weights obtained from Eq. (1) for the corresponding values of R_1 and R_2. They set the limits on the molecular weight region where the exclusion becomes total in relation to capillaries with radius R_1. In this zone, for a fixed MW value, the calculated retention times for the network model are lower than the retention times for the parallel bundle. As expected, this indicates that the parallel bundle accessibility for those exclusion conditions is higher than the accessible pore volume of the network.

The analysis of the band broadening mechanism is more complex. Figure 6 shows the standard deviations (SD) of the computed elution curves in terms of the polymer molecular weight for different values of F1 for the parallel bundle pore structure. The predicted maximum value for SD is a well known effect [1]. It results from the competition between the exclusion and the hindered diffusion mechanism in the intraparticle pores. This is also predicted by the network model and the results are shown in Figure 7. However, for a fixed MW, the band broadening in terms of the structural parameter F1 is not of the general pattern found for parallel bundles. Whereas the results plotted in Figure 6 show a monotonic behaviour for the calculated SD values with respect to F1, the network results shown in Figure 7 give evidence of a maximum in SD values around a frequency F1 equal to 0.75. At this F1 value, the predicted tortuosity factors for randomly generated square networks are notably high [13]. This is a consequence of the mass transfer control of the large pores governed by the frequency (1-F1) and spatial distribution of pore sizes equal to R_2 in the network.
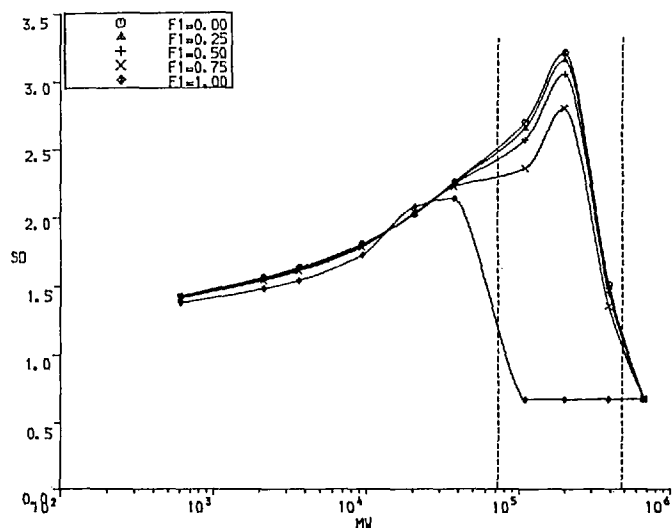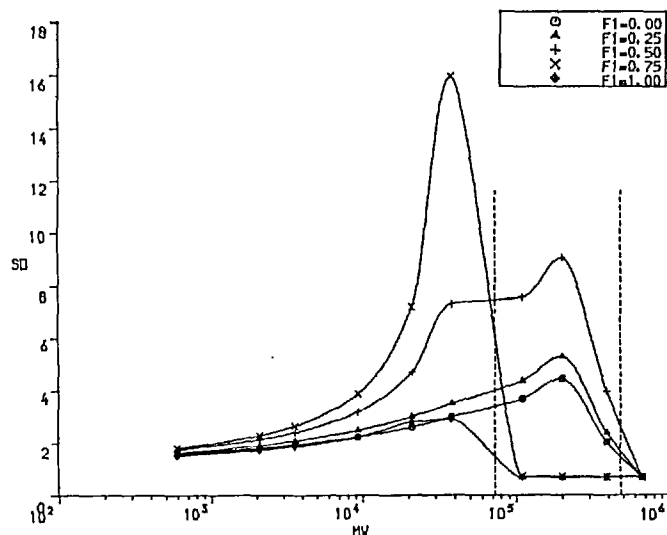
Figure 7

Dependence of the standard deviation on the polymer molecular weight for the network model (SD in minutes).

Figure 8

Degree of scattering of the standard deviation at F1 = 0.25 for the network model (SD in minutes).

Figure 6

Dependence of the standard deviation on the polymer molecular weight for the parallel bundle model (SD in minutes).
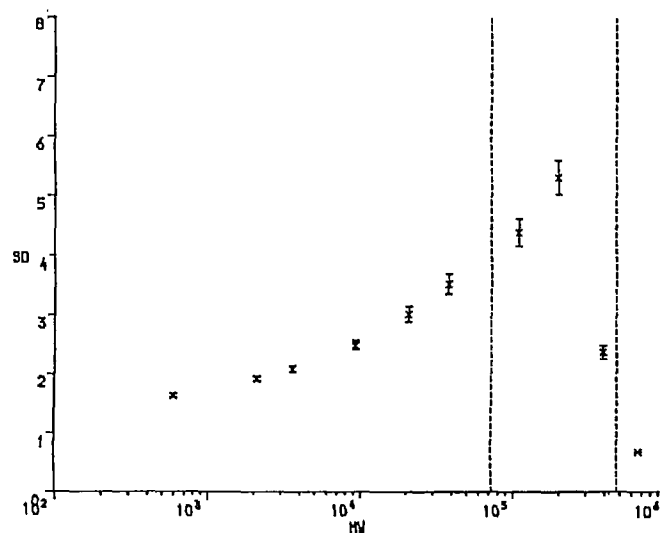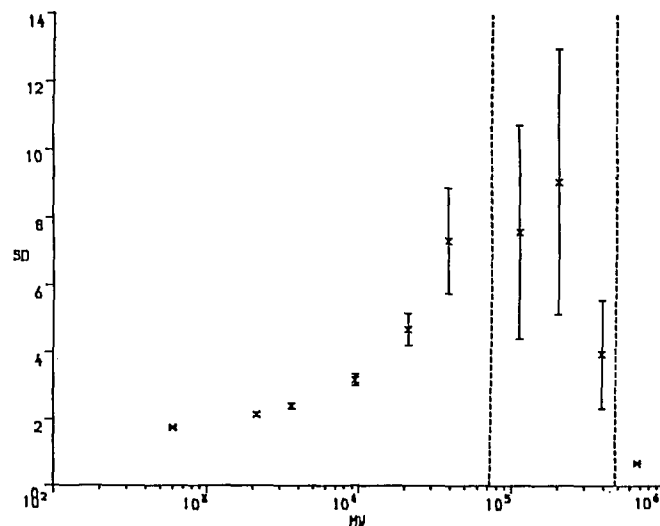
Figure 9

Degree of scattering of the standard deviation at F1 = 0.5 for the network model (SD in minutes).
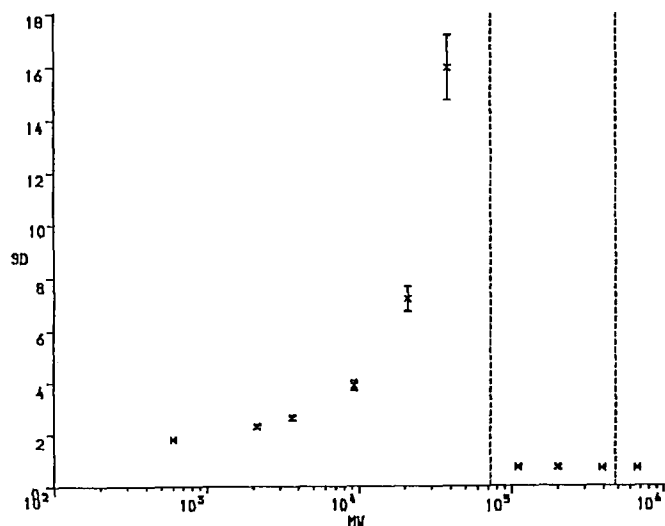
Figure 10

Degree of scattering of the standard deviation at F1 = 0.75 for the network model (SD in minutes).

Figures 8, 9 and 10 show the degree of scatter arising from the sampling procedure for a given value of F1. At F1 = 0.5 (Figure 9) the calculated SD for the eluted chromatographic peak fluctuates widely in the zone where the exclusion mechanism for capillaries with small radius is total, i.e. in the domain bounded by the dashed lines in the figures. This frequency is known as the *percolation threshold* for the square network [14] and the large uncertainty is directly related to the critical conditions in which the network samples have been generated.

Conclusions

A network model for SEC has been developed and compared with a conventional pore volume model based on a parallel bundle of capillaries. It is shown that the pore volume morphology can have a very strong influence on the band broadening behaviour of SEC columns. Spatial non-uniformities have been generated in a systematic manner so that the concept of a network tortuosity factor [13] can be employed to elucidate the structural influence.

The approach to modelling presented in this work offers a useful methodology for the specification and design of the SEC column packings. It also points to a means of using size exclusion chromatography with standard polymeric samples to characterize the porous structure of SEC column packings.

Acknowledgement

Symbols

C_m — transformed mobile phase concentration

$\bar{c}$ — transformed capillary concentration

$\bar{C}_m$ — mobile phase concentration ($\overline{mol}/cm^3$)

$\bar{c}$ — capillary concentration (mol/cm^3)

D_m^0 — molecular diffusion coefficient (cm^2/s)

D_m — hindered diffusion coefficient (cm^2/s)

D_L — dispersion coefficient (cm^2/s)

F1 — frequency of the smaller radius

J — transformed molar flux

$\bar{J}$ — molar flux (mol/s)

L — column length (cm)

l — network capillary length (cm)

l_p — particle size (cm)

N — network dimension

R — pore radius (cm)

s — transformed variable

t — time (s)

$\langle v \rangle$ — interstitial velocity (cm/s)

V_{PS} — internal volume of the particle (cm^3)

X — column axial coordinate (cm)

x — capillary axial coordinate (cm)

Subscripts

i — related to node i

j — related to node j

Greek Symbols

ε_c — column porosity

ε_p — particle porosity

ϕ — distribution coefficient

μ — moment of the residence time distribution

References

[1] W. W. Yau, J. J. Kirkland, D. D. Bly, "Modern Size-Exclusion Liquid Chromatography", John Wiley & Sons, New York, 1979; chapters 1, 2 and 3.

[2] J. J. Hermans, J. Polymer Sci. A6, 1217 (1968).

[3] A. C. Ouano, J. A. Barker, Separ. Sci. 8, 673 (1973).

[4] M. Kubin, J. Chromatogr. 108, 1 (1975).

[5] W. M. Deen, AIChE J. 33, 1409 (1987).

[6] C. N. Satterfield, C. K. Colton, W. II. Pitcher, AIChE J. 19, 628 (1973).

[7] C. K. Colton, C. N. Satterfield, C. Lai, AIChE J. 21, 289 (1975).

[8] M. Sahimi, V. L. Jue, AIChE Symp. Ser. 84 (266), 40 (1988).

[9] M. Sahimi, V. L. Jue, Phys. Rev. Lett. 62, 629 (1989).

[10] R. N. Kelley, F. W. Billmeyer, Jr., Anal. Chem. 41, 874 (1969).

[11] J. R. Pappenheimer, E. M. Renkim, L. M. Barrero, Am. J. Physiol. 67, 13 (1951).

[12] J. Villadsen, M. L. Michelsen, "Solution of Differential Equation Models by Polynomials Approximation", Prentice Hall Inc.: Englewood Cliffs, NJ, 1978; chapter 3.

[13] K. Rajagopal, J. S. Andrade Jr., C. McGreavy, to be published.

[14] K. K. Mohanty, J. M. Ottino, H. T. Davis, Chem. Eng. Sci. 37, 905 (1982).